

PAPER

Surface recombination velocity on wet-cleaned silicon wafers using heterodyne lock-in carrierography imaging: measurement uniqueness investigation

To cite this article: Peng Song *et al* 2020 *Semicond. Sci. Technol.* **35** 055013

View the [article online](#) for updates and enhancements.

Recent citations

- [Fully nonlinear photocarrier radiometry / modulated photoluminescence dynamics in semiconductors: Theory and applications to quantitative deconvolution of multiplexed photocarrier density wave interference and recombination processes](#)
Qiming Sun *et al*

- [Lock-in carrierography non-destructive imaging of silicon wafers and silicon solar cells](#)
Peng Song *et al*

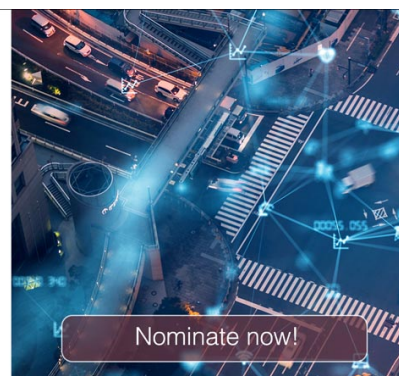


The Electrochemical Society
Advancing solid state & electrochemical science & technology

The ECS is seeking candidates to serve as the **Founding Editor-in-Chief (EIC) of ECS Sensors Plus**, a journal in the process of being launched in 2021

The goal of ECS Sensors Plus, as a one-stop shop journal for sensors, is to advance the fundamental science and understanding of sensors and detection technologies for efficient monitoring and control of industrial processes and the environment, and improving quality of life and human health.

Nomination submission begins: May 18, 2021



Surface recombination velocity on wet-cleaned silicon wafers using heterodyne lock-in carrierography imaging: measurement uniqueness investigation

Peng Song^{1,2} , Alexander Melnikov² , Qiming Sun² ,
Robert H Pagliaro³ , Xiaogang Sun¹, Junyan Liu^{4,5,6} and
Andreas Mandelis^{2,6}

¹ School of Instrumentation Science and Engineering, Harbin Institute of Technology, Harbin, 150001, People's Republic of China

² Center for Advanced Diffusion-Wave and Photoacoustic Technologies (CADIPT), University of Toronto, Toronto, M5S 3G8, Canada

³ Advanced Processing Equipment Technology (APET) Co., Ltd, 20-15, Sukwoo-Dong, Hwaseong-City, Gyeonggi-do 463-802, Republic of Korea

⁴ School of Mechatronics Engineering, Harbin Institute of Technology, Harbin, 150001, People's Republic of China

⁵ State Key Laboratory of Robotics and System, Harbin Institute of Technology, Harbin, 150001, People's Republic of China

E-mail: ljywlj@hit.edu.cn and mandelis@mie.utoronto.ca

Received 24 December 2019, revised 11 February 2020

Accepted for publication 19 February 2020

Published 31 March 2020



CrossMark

Abstract

Characterization of semiconductor surface quality is important for evaluating the surface preparation methods. In this work, three wet-cleaned silicon wafers with different surface conditions were inspected using heterodyne lock-in carrierography (HeLIC) imaging simultaneously with homodyne photocarrier radiometry (HoPCR). The surface recombination velocity was measured at various queue times after the wet-clean treatment using HeLIC and was found to be consistent with values obtained using HoPCR. The results show that HeLIC can provide a reliable quantitative imaging tool for evaluating the surface conditions of wet-cleaned silicon wafers.

Keywords: lock-in carrierography, photocarrier radiometry, surface recombination velocity, silicon wafers, homodyne, heterodyne

(Some figures may appear in colour only in the online journal)

1. Introduction

Wet-cleaned chemical methods are widely used for surface preparation in the semiconductor silicon industry. Characterization of the surface quality prior to device processing is important for evaluating the surface preparation methods. Surface recombination velocity (SRV) is a critical parameter

in silicon device applications including solar cells [1, 2]. A number of advanced optical techniques have been developed to measure or determine the SRV of silicon wafers and silicon solar cells, such as photoconductance decay [3] and photoluminescence [4, 5]. Since the size of state-of-the-art wafers has already reached 300 mm, spatially resolved changes in the surface quality of wafers are more relevant than surface-averaged quality measurements and thus camera-based methods to obtain SRV images are in high demand.

⁶ Authors to whom any correspondence should be addressed.

Lock-in carrierography/photoluminescence (LIC/LIPL) [6], an imaging counterpart of photocarrier radiometry (PCR) [7], is a frequency-domain photoluminescence (PL)-based quantitative characterization method. The advantages of LIC are that it is contactless and calibration-free. Since LIC employs the lock-in algorithm, it has a better signal-to-noise ratio (SNR) than PL and can measure kinetic parameters in semiconductors as a dynamic (non-static) modality. It has been used to characterize electronic transport parameters (bulk lifetime, diffusion coefficient and SRV) [8–10] and electrical parameters (saturation current density, open-circuit voltage, fill factor and so on) in semiconductor materials and devices [11–13].

To achieve high-frequency imaging using an InGaAs camera with 100 Hz limited frame rate, heterodyne lock-in carrierography (HeLIC) was introduced. HeLIC employs two modulation frequencies and has been used to characterize the performance of silicon substrates [14, 15]. Very recently, HeLIC was employed to simultaneously determine the bulk lifetime and SRV of wet-cleaned silicon wafers under the assumptions of known diffusion coefficient and fixed bulk lifetime, while surface processing conditions were varied [16].

However, unlike homodyne PCR, HeLIC uses the heterodyne amplitude as the only effective signal because the heterodyne phase across all frequencies is close to 0° . Homodyne photocarrier radiometry (HoPCR) was used to supplement quantitative HeLIC imaging [9] as it produces not only amplitude but also the phase signals and thus can resolve the bulk lifetime (less than 100 ms), SRV, and diffusion coefficient [17]. It was found that the reliability and uniqueness of HeLIC as a method to resolve the bulk lifetime, the SRV, and the diffusion coefficient could be supplemented using HoPCR [9]. As an advance over the prior combined HoPCR and HeLIC studies, in the present work HeLIC was found to reliably and uniquely determine the SRV on wet-cleaned silicon wafers alone without any assumptions and any supplementary methods. Toward this goal, SRV imaging of wet-cleaned silicon wafers with three different surface preparation methods was carried out using HeLIC simultaneously with HoPCR. Furthermore, HeLIC was also used to monitor SRV changes of treated silicon wafers in air with various exposure times ('queue-time' or 'Q-time').

2. Experimental apparatus and procedures

2.1. Materials

Three p-type (B-doped) float-zone silicon wafers with resistivity over 10 k Ω cm from the same batch labeled as Sample I, Sample II and Sample III were investigated in this work. All three samples were 680 μ m thick and 150 mm in diameter. Sample I was processed using a TeraDoxTM wet-cleaning method developed by Advanced Processing Equipment Technology (APET) [18], featuring 100:1 HF acid with a 100-ppt dissolved oxygen (DO) level. Sample II was processed with a typical production wet bench using 100:1 HF

with a 2 ppm DO level (not degassed). Sample III was etched with an in-house wet bench using 2% HF (not degassed).

2.2. Experimental technique

2.2.1. Principles. The principles of PCR/LIC in homodyne and heterodyne modalities have already been described elsewhere [9]. Briefly, PCR employs a single-element detector to evaluate the photogenerated carrier density wave while LIC employs a camera instead of the single-element detector. In the homodyne mode, a sample is excited using a single laser modulation frequency, while in the heterodyne mode the sample is excited using two adjacent laser frequencies and the detector captures the generated beat envelope wave. Transport parameters such as SRV are extracted from experimental PCR/LIC data by best-fitting to relevant theoretical models.

The excess carrier density wave $\Delta n(z)$ generated by means of a homogenized laser beam was determined from the one-dimensional carrier diffusion equation [19, 20].

$$D^* \frac{\partial^2 \Delta n(t, z)}{\partial z^2} - \frac{\Delta n(t, z)}{\tau_b} - \frac{\partial \Delta n(t, z)}{\partial t} = -G_0 \beta e^{-\beta z} g(t), \quad (1)$$

where D^* is the carrier diffusion coefficient, τ_b the bulk lifetime, G_0 the average optical generation rate, β the optical absorption coefficient and $g(t)$ the forcing function.

The frequency-domain solution $\Delta n(\omega, z)$ of equation (1) can be expressed as

$$\Delta n(\omega, z) = C_1 e^{-\sigma z} + C_2 e^{-\sigma(L-z)} - \frac{G_0 \beta}{D(\beta^2 - \sigma^2)} e^{-\beta z}, \quad (2)$$

where $\sigma = [(\tau_b^{-1} + i\omega)/D^*]^{1/2}$, L is the wafer thickness, and C_1, C_2 are constants determined from the third kind boundary conditions

$$\begin{aligned} D^* \frac{d\Delta n(\omega, x)}{dx} \Big|_{x=0} &= S_f \Delta n(\omega, x=0), \\ D^* \frac{d\Delta n(\omega, x)}{dx} \Big|_{x=L} &= -S_r \Delta n(\omega, x=L), \end{aligned} \quad (3)$$

where S_f and S_r are the surface recombination velocities for front and rear surface, respectively. Here, the front and rear surface recombination velocities were assumed to be the same, i.e. $S_f = S_r \equiv s$, reflecting identical treatment conditions of both surfaces by the manufacturer.

The linearized homodyne PCR/LIC signal can be expressed in the form

$$S_{\text{Ho}}(\omega) = C \int_0^L \Delta n(\omega, z) dz, \quad (4)$$

where C is a proportionality factor.

The linearized heterodyne PCR/LIC signal can be expressed as

$$S_{\text{He}}(\Delta\omega) = C_{\text{in}} \int_0^L \Delta n(-\omega_1, z) \Delta n(\omega_2, z) dz, \quad (5)$$

where $\Delta\omega = |\omega_2 - \omega_1|$ and C_{in} is a proportionality constant. Here, $\Delta n(-\omega_1, z) = \Delta n^*(\omega_1, z)$, where $*$ denotes complex

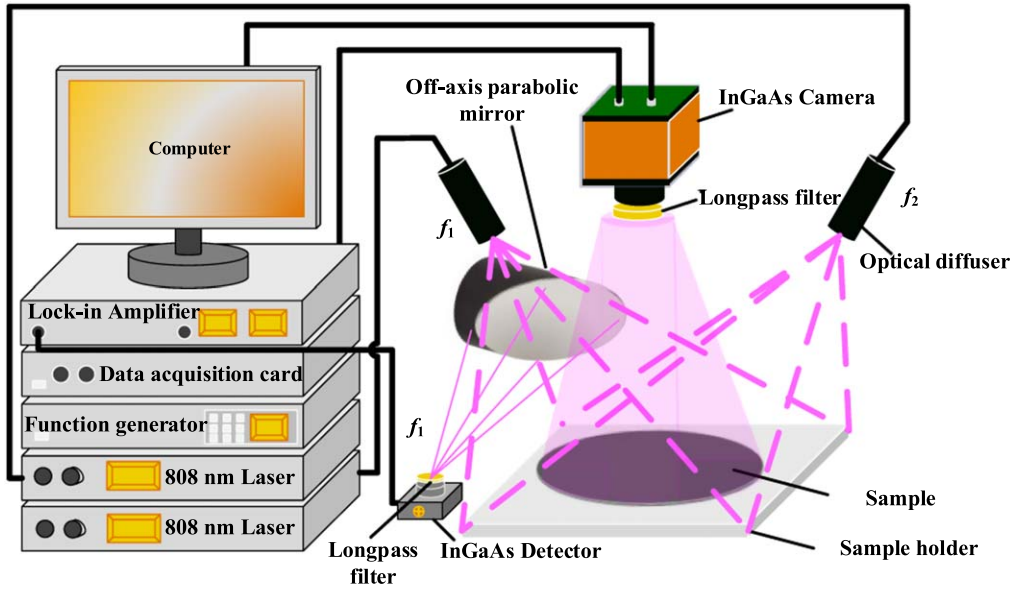


Figure 1. Experimental setup for combined lock-in carrierography and photocarrier radiometry.

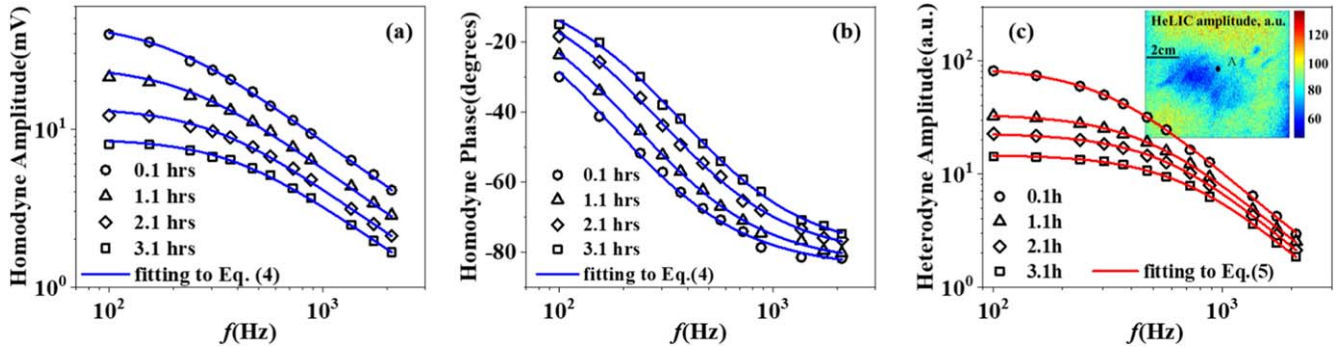


Figure 2. HoPCR amplitude (a) and phase (b) at point A of Sample I and their best-fits to equation (4), simultaneously with (c) the HeLIC amplitude-frequency response and best-fits to equation (5). The inset in figure 2(c) is a heterodyne amplitude image at $f_1 = 100$ Hz and Q-time 0.1 h.

conjugation; this indicates the nonlinear frequency mixing nature of the beat-frequency detection operation inherent in heterodyne signals.

To improve the accuracy of fitting results, the values of C and C_{in} can be determined during the fitting process in the following equation:

$$C, C_{in} = \frac{1}{n} \sum_{i=1}^n \frac{S_{Calculation}^i}{S_{Experiment}^i}, \quad (6)$$

where $S_{calculation}$ stands for the calculated values, $S_{experiment}$ for the experimental values, n is the number of experimental data.

2.2.2. Apparatus. An experimental combined HeLIC and PCR setup is shown in figure 1. The HeLIC system mainly features two 45 W, 808 nm laser diode sources, a two-channel function generator, and an InGaAs camera. The lasers were sine-wave modulated with frequencies f_1 and $f_2 = f_1 + 2$ Hz using the two-channel function generator. The laser beams were collimated, homogenized, and spread by a microlens array which made the illumination area up to $100 \times 100 \text{ mm}^2$

Table 1. Surface recombination velocity of Sample I obtained by means of HoPCR and HeLIC at early Q-times.

Q-time (h)	SRV (m s^{-1}) (HoPCR)	SRV (m s^{-1}) (HeLIC)
0.1	0.31	0.24
1	0.42	0.43
2	0.62	0.65
3	0.82	0.82

and the mean intensity of each laser beam up to 100 mW cm^{-2} . PL signals at the fundamental frequencies (f_1 and f_2), beat frequency (Δf) and sum frequency ($f_1 + f_2$) were generated when the sample was excited at the two laser frequencies. An InGaAs camera (bandwidth: $0.9\text{--}1.7 \mu\text{m}$, 320×256 pixels, frame rate up to 60 Hz) was employed to capture HeLIC amplitude (beat frequency) signals. A longpass filter (LP-1000 nm) mounted in front of the camera was used to block the excitation laser beams. A data acquisition card (NI USB-6259) was used to generate a reference signal (2 Hz) and external trigger to the camera in a synchronous

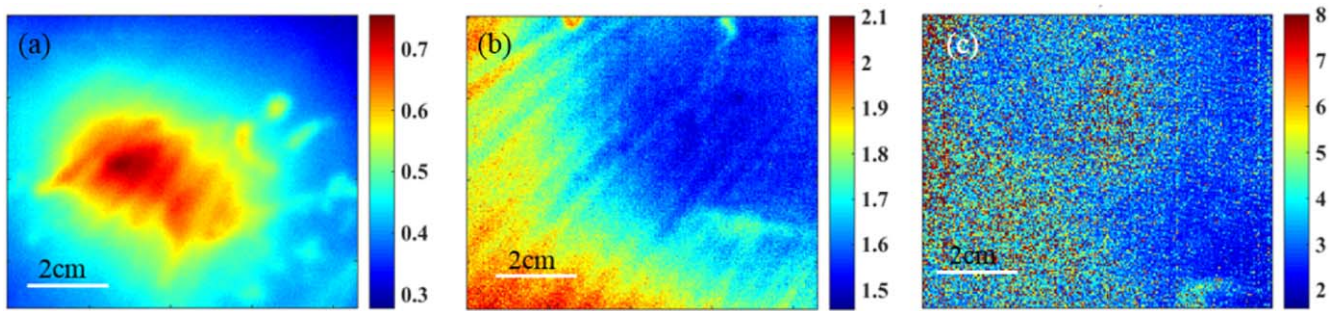


Figure 3. Best-fitted surface recombination velocity images at early Q-times of (a) Sample I, (b) Sample II, and (c) Sample III. The color bar SRV units in these figures are m s^{-1} .

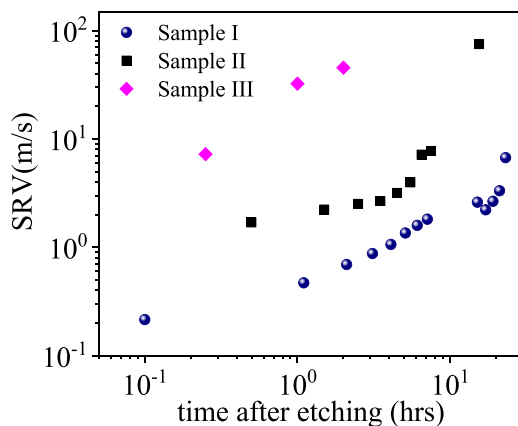


Figure 4. Dependencies of image-averaged SRV of the three samples on time after wet cleaning.

oversampling mode. A single-element InGaAs detector with a long-pass filter was employed to measure the amplitude and phase of the homodyne signal at f_1 in the PCR system. A lock-in amplifier was used to demodulate the signals from the detector at f_1 . In our system, the detector and camera recorded the HoPCR and HeLIC signals simultaneously. The aforementioned three samples were measured in sequence using this system.

3. Experimental results and discussion

Transport parameters were extracted by fitting the frequency dependences of amplitude and phase signals to corresponding theoretical models [7, 15]. The frequency dependence of sample I at point A of HoPCR amplitude and phase, and HePCR amplitude, and their best-fits to corresponding theoretical models at various Q-times are shown in figure 2. The inset in figure 2(c) is a heterodyne amplitude image of that sample at $f_1 = 100$ Hz. From figure 2, it can be seen that the amplitude and phase lag decreased with increasing Q-time under the same illumination intensity. The change was mainly induced by electronically deteriorating surface conditions with Q-time [16]. Our measurement results showed that HeLIC was not capable of resolving all transport parameters

simultaneously when the bulk lifetime was comparable with the surface lifetime (τ_s) because the only signal available was the effective heterodyne amplitude [9]. Surface lifetime is a function of the surface recombination velocities, the minority carrier diffusivity and the wafer thickness [21]. One can calculate τ_s with known SRVs⁷. When the wafer thickness is $680 \mu\text{m}$ and $s = 10 \text{ cm s}^{-1}$, the τ_s changes from 3.86 to 3.41 ms with the minority carrier diffusivity varying from 1 to $36 \text{ cm}^2 \text{ s}^{-1}$. From this calculation, it can be seen that the minority carrier diffusivity has less influence on surface lifetime under this condition. If the bulk lifetime is much higher than the surface lifetime, then the SRV can be resolved. On the other hand, if the bulk lifetime is much shorter than the surface lifetime, the former can be resolved. In our case, the SRV could be resolved using HeLIC. To verify the uniqueness of the SRV values obtained from HeLIC, the SRVs were also derived simultaneously from PCR amplitude and phase signals and are shown in table 1. It is seen that for the first three hours, the SRV obtained from HeLIC and HoPCR are very consistent with each other.

Figure 3 shows the HeLIC SRV images of the three investigated samples at very early Q-times. It was found that the SRV values of Sample I were the lowest (average value: 0.47 m s^{-1}) among the three samples due to the lowest DO level in the wet-clean chemistry, while those of Sample III were the highest (average value: 7.23 m s^{-1}), as expected due to the highest DO level [16]. Thus, the TeraDoxTM wet cleaning solution was shown to provide superior (i.e. more H-passivated [22]) surface conditions for wafer fabrication processing. Figure 3 also reveals inhomogeneities in the three samples and can be used as a guide to improve the surface and the entire substrate quality.

The SRVs of the three samples averaged over whole SRV images, figure 3, at various Q-times are shown in figure 4. Comparing the results, the mean SRV of Sample I was found to be the lowest, followed by that of Sample II and sample III at the same Q-time. The SRVs of the three samples were found to increase with exposure time due to the degradation of surface (passivation) quality [23]. These trends follow closely the detailed SRV distribution images of

⁷ See <https://pveducation.org/pvc/drom/characterisation/surfacerecombination> for surface recombination.

figure 3 and lead to the conclusion that sample I exhibits a relatively slow SRV growth rate which indicates that the surface conditions when wet cleaned with TeraDox™ are better and more stable than the surfaces cleaned with the conventional methods following exposure to ambient air. It can thus be concluded that the TeraDox™ wet cleaning process provided the best surface-wide wafer quality among these samples. The TeraDox™ wet cleaning process could provide a silicon wafer SRV as low as 0.21 m s^{-1} under the 100:1 HF condition.

4. Conclusions



Homodyne photocarrier radiometry (HoPCR) with amplitude and phase signals was used to verify the uniqueness of SRV images of three wet-cleaned silicon wafers under various wet-clean surface treatment methods obtained with Heterodyne lock-in carrierography (HeLIC). The results showed that SRVs obtained with HeLIC were in good agreement with those obtained with HoPCR. HeLIC imaging was found to be able to reliably resolve the SRV of the wet-cleaned silicon wafers. Silicon wafers which underwent the TeraDox™ treatment exhibited the lowest SRV values (0.21 m s^{-1}) and the slowest post-clean (Q-time) growth rate in ambient air.

Acknowledgments

AM is grateful to the Natural Sciences and Engineering Research Council of Canada (NSERC) for a Discovery grant and to the Canada Research Chairs Program. JL is grateful to the Foundation for Innovative Research Groups of the National Nature Science Foundation of China (Grant No. 51521003), to the Natural Science Foundation of China (Contract No. 61571153), and to the Program of Introducing Talents of Discipline of Universities (Grant No. B07108).

ORCID iDs

Peng Song  <https://orcid.org/0000-0002-6029-945X>
Alexander Melnikov  <https://orcid.org/0000-0002-0020-9862>

Qiming Sun  <https://orcid.org/0000-0003-1184-3719>
Robert H Pagliaro  <https://orcid.org/0000-0003-3437-7829>

References

- [1] Basher M K, Hossain M K and Akand M A R 2019 *Optik* **176** 93–101
- [2] Basher M K, Mishan R, Biswas S, Hossain M K, Akand M A R and Matin M A 2019 *AIP Adv.* **9** 075118
- [3] Ahrenkiel R K and Johnston S W 2009 *Sol. Energy Mater. Sol. Cells* **93** 645–9
- [4] Baek D, Rouvimov S, Kim B, Jo T C and Schroder D K 2005 *Appl. Phys. Lett.* **86** 112110
- [5] Heinz F D, Warta W and Schubert M C 2017 *Appl. Phys. Lett.* **110** 042105
- [6] Melnikov A, Mandelis A, Tolev J, Chen P and Huq S 2010 *J. Appl. Phys.* **107** 114513
- [7] Mandelis A, Batista J and Shaughnessy D 2003 *Phys. Rev. B* **67** 205208
- [8] Sun Q, Melnikov A and Mandelis A 2012 *Appl. Phys. Lett.* **101** 242107
- [9] Song P, Melnikov A, Sun Q, Mandelis A and Liu J 2019 *J. Appl. Phys.* **125** 065701
- [10] Song P, Melnikov A, Sun Q, Mandelis A and Liu J 2018 *Semicond. Sci. Technol.* **33** 12LT01
- [11] Liu J, Melnikov A and Mandelis A 2013 *J. Appl. Phys.* **114** 104509
- [12] Zhang Y, Melnikov A, Mandelis A, Halliop B, Kherani N P and Zhu R 2015 *Rev. Sci. Instrum.* **86** 033901
- [13] Hu L, Liu M, Mandelis A, Melnikov A and Sargent E H 2017 *Prog. Photovolt. Res. Appl.* **25** 1034
- [14] Melnikov A, Chen P, Zhang Y and Mandelis A 2012 *Int. J. Thermophys.* **33** 2095
- [15] Sun Q, Melnikov A and Mandelis A 2016 *Phys. Status Solidi A* **213** 405–11
- [16] Sun Q, Melnikov A, Mandelis A and Pagliaro R H 2018 *Appl. Phys. Lett.* **112** 012105
- [17] Li B, Shaughnessy D and Mandelis A 2005 *J. Appl. Phys.* **97** 023701
- [18] <http://apet.co.kr>
- [19] Mandelis A 2001 *Diffusion-Wave Fields Mathematical Methods and Green Functions* (New York: Springer) p 586
- [20] Giesecke J A, Kasemann M, Schubert M C, Würfel P and Warta W 2010 *Prog. Photovolt. Res. Appl.* **18** 10–9
- [21] Luke K L and Cheng L J 1987 *J. Appl. Phys.* **61** 2282–93
- [22] Trucks G W, Raghavachari K, Higashi G S and Chabal Y J 1990 *Phys. Rev. Lett.* **64** 504–7
- [23] Pointona A I, Granta N E, Wheeler-Jones E C, Altermatt P P and Murphy J D 2018 *Sol. Energy Mater. Sol. Cells* **183** 164–72